**Indonesian Journal of Material Research**
*e*-ISSN: 2987-1654
Vol. 3, No. 3, November 2025

Indonesian Journal of MATERIAL RESEARCH

Research Paper

# Comparative Assessment of Procion Red Removal Using Magnetite-Based Composites with Humic Acid, Activated Charcoal, and Lignin

Nur Ahmad[1*], Alfan Wijaya[1,2], Amri[1,2]

[1] *Research Center of Inorganic Materials and Coordination Complexes, Universitas Sriwijaya, Palembang, 30139, Indonesia*
[2] *Doctoral Program of Environmental Sciences, Graduate School of Universitas Sriwijaya, Palembang, 30139, Indonesia*
[*]**Corresponding author**: nurahmadtula23@gmail.com

**Abstract**
This investigation presents the synthesis and comparative assessment of three magnetite-based composite adsorbents, including Magnetite Humic Acid (MA), Magnetite Activated Charcoal (MB), and Magnetite Lignin (MC), aimed to remove Procion Red (PR) from aqueous solutions. The characterization of the materials was conducted through XRD, BET, and FTIR analyses, which validated the successful synthesis of magnetite and its interactions with the respective organic components. The point of zero charge (pHpzc) values obtained were 4.75, 5.09, and 4.10 for MA, MB, and MC, respectively. Adsorption experiments were performed under these pHpzc conditions to mitigate electrostatic influences. Kinetic investigations demonstrated that the adsorption process adhered to a pseudo-second-order model, signifying that chemisorption was the prevailing mechanism. Furthermore, the Langmuir isotherm yielded the most accurate representation of the equilibrium data, implying the occurrence of monolayer adsorption. MB demonstrated the highest adsorption capacity of PR, recorded at 52.632 mg/g at a temperature of 50°C. This observation underscores the benefits associated with its elevated surface area and the effective dispersion of $Fe_3O_4$ particles within the activated carbon matrix. The comparative analysis elucidates the impact of organic matrix selection on surface characteristics, interaction dynamics, and the overall efficacy of adsorption processes. This study presents novel findings regarding the development of natural carbon-magnetite composites aimed at enhancing the efficiency of dye removal processes.

**Keywords**
Adsorption, Magnetite, Charcoal Activated, Humic Acid, Lignin

Received: 13 July 2025, Accepted: 8 October 2025
https://doi.org/10.26554/ijmr.20253368

## 1. INTRODUCTION

The release of wastewater containing dyes from textile manufacturing poses a significant environmental challenge, attributed to the enduring nature, toxicity, and aesthetic detriment associated with synthetic dyes (Mohd Nor et al., 2015; Ribas et al., 2020). Procion red (PR), classified as a reactive azo dye, is extensively utilized in the dyeing of cellulose fibers among the diverse array of synthetic dyes available (Anuar et al., 2020; Tao and Wang, 2023). Nonetheless, it exhibits significant solubility in aqueous solutions and demonstrates resistance to biodegradation, resulting in its accumulation within aquatic ecosystems (Sarma et al., 2018). PR, even at minimal concentrations, has the potential to markedly diminish light penetration in aquatic environments, interfere with photosynthetic activities, and induce ecological disturbances. Furthermore, the degradation products associated with this compound exhibit mutagenic and carcinogenic properties, thereby presenting significant long-term risks to both human health and aquatic ecosystems (Iqajtaoune et al., 2024).

Previous approaches for the removal of dyes from wastewater include techniques such as coagulation-flocculation, membrane filtration, photodegradation, and biological treatment (Cotillas et al., 2018; Palas et al., 2016). Although these methodologies can result in partial decolorization, they each exhibit considerable limitations. The processes of coagulation and flocculation result in the production of substantial quantities of secondary sludge, which necessitates additional disposal measures. Membrane filtration is hindered by issues related to membrane fouling and elevated operational expenses. Photodegradation relies on intense light sources and demonstrates reduced efficacy when applied to colored or turbid effluents. Furthermore, biological treatment methods exhibit limitations in addressing non-biodegradable dyes, exemplified by PR. Conversely, adsorption has been recognized as a straightforward, efficient, and economically viable method capable of eliminating dyes, even at low concentrations, while avoiding the generation of detrimental byproducts (Wijaya et al., 2023; Salman et al., 2022; Thue et al., 2024). The primary benefits encompass the reusability of the adsorbent, operational simplicity, and suitability for large-scale industrial applications, positioning it as a highly promising method for the treatment of

textile dye wastewater (Palapa and Wijaya, 2023; Wijaya et al., 2021).

Magnetite ($Fe_3O_4$) has garnered significant interest in recent years as an adsorbent, attributed to its extensive surface area, robust chemical stability, and the convenience of separation through an external magnetic field, facilitating swift recovery and subsequent reuse (Kalidason and Kuroiwa, 2022; Ain et al., 2024). Nonetheless, the aggregation of pure magnetite nanoparticles is a prevalent issue, which subsequently diminishes their active surface area and adsorption efficiency. The surface chemistry of these materials presents a constrained availability of functional groups for interaction with dye molecules, thereby limiting their adsorption capacity. In response to these limitations, investigations have led to the formulation of magnetite composites incorporating carbon-based materials, including humic acid, activated charcoal, and lignin (Ahmad et al., 2024). The natural modifiers in question exhibit a high density of oxygen-containing functional groups, including carboxyl (-COOH), hydroxyl (−OH), and carbonyl (−C=O) moieties (Amri et al., 2024; Hingrajiya and Patel, 2023; Li et al., 2024). These functional groups significantly enhance surface reactivity, thereby promoting electrostatic interactions, hydrogen bonding, and $\pi$-$\pi$ interactions with various dye molecules. Moreover, the integration of these natural carbon materials contributes to the improved stability, dispersibility, and environmental compatibility of magnetite (Ayesha et al., 2023). Notwithstanding the increasing body of research, a comprehensive comparative analysis of these three categories of magnetite-carbon composites under uniform conditions is still lacking.

Therefore, this study seeks to synthesize and evaluate the adsorption capabilities of Magnetite Humic Acid (MA), Magnetite Activated Charcoal (MB), and Magnetite Lignin (MC) in the context of PR removal from aqueous solutions. The characterization of each composite was performed utilizing X-ray diffraction (XRD), Fourier-transform infrared spectroscopy (FTIR), and Brunauer-Emmett-Teller (BET) analysis to elucidate structural and surface properties. Additionally, adsorption experiments were executed at the corresponding point of zero charge (pHpzc) values to evaluate the intrinsic adsorption behavior. This research further examines the kinetics of adsorption and isotherm models to clarify the underlying mechanisms and assess the impact of natural modifiers on dye uptake and surface interactions, thereby offering significant insights for the development of effective and sustainable dye adsorbents.

## 2. EXPERIMENTAL

### 2.1 Chemicals

All chemicals employed in this investigation were of analytical grade and utilized without additional purification. PR served as the model anionic dye for the assessment of adsorption performance. Throughout all experimental procedures, distilled water was employed for the preparation of solutions and for washing steps. Stock dye solutions at a concentration of 1000 mg/L were formulated by dissolving a precisely measured quantity of PR in distilled water, followed by dilution to achieve the specified concentrations. The pH of all solutions was meticulously adjusted utilizing 0.1 M HCl and 0.1 M NaOH as necessary.

### 2.2 Preparation of Magnetite Composite

The synthesis of magnetite is conducted through the combination of $FeCl_3$ and $FeSO_4.7H_2O$ compounds in varying molar ratios of 2:1, with each component being dissolved in 3 mL of distilled water, followed Ahmad et al. (2025) synthesis method. The two solutions are subsequently combined and agitated with a stirrer for a duration of 10 min. Subsequently, 1 g of humic acid, lignin, and activated charcoal is introduced into the mixture and agitated with a stirrer for a duration of 3 h. Subsequently, 3.5 mL of a 25% ammonia solution is administered gradually into the mixture while maintaining a temperature of 75°C. The sample is subjected to hydrothermal conditions at a temperature of 150°C for a duration of 3 h. Subsequently, the mixture undergoes filtration and is subjected to washing with distilled water, followed by drying in an oven maintained at a temperature of 100°C. The synthesized materials are labeled as MA for magnetite humic acid, MB for magnetite activated charcoal, and MC for magnetite lignin.

### 2.3 PR adsorption in MA, MB, and MC Material

The impact of adsorption time was examined by subjecting the adsorbent to the adsorbate dye at multiple contact intervals, specifically 0, 10, 20, 30, 40, 50, 70, 90, 120, 150, and 180 min under pHpzc conditions. The procedure involved the placement of 20 mL of each preparation of 50 mg/L of PR into individual beakers for observation. Subsequently, 20 mg of the synthesized material was incorporated as the adsorbent. The mixture underwent stirring with a shaker at different contact durations, followed by separation utilizing an external magnet. The filtrate was subsequently analyzed for absorbance at the wavelength corresponding to maximum absorbance, utilizing a UV-Vis spectrophotometer. The absorbance of the dye obtained was systematically plotted to enable subsequent analysis. Investigations were undertaken to assess the influence of temperature, varying from 30 to 50°, on an initial concentration of 50 mg/L of PR.

## 3. RESULTS AND DISCUSSION

The X-ray diffraction (XRD) patterns, in Figure 1, observed for samples MA, MB, and MC exhibit broad peaks within the $2\theta$ range of 20-23° corresponding to the (002) plane of carbon (dos Santos et al., 2021). The presence of these broad peaks suggests the amorphous characteristics of the carbon material, which is indicative of the complex and irregular structure inherent in natural organic materials, thereby signifying low crystallinity. The diffraction pattern of magnetite exhibits distinct sharp peaks at $2\theta$ values of 30.28° (200), 35.58° (311), 43.23° (400), 53.76° (422), 57.24° (522), and 62.84° (440), in accordance with JCPDS No. 96-900-5840 (Naik and Thakur, 2024). The observation of these peaks substantiates the successful synthesis of the magnetite phase across all composite samples. The observed peak intensities for MA and MC are slightly lower in comparison to MB, suggesting that the presence of humic acid and lignin contributes to

a reduction in crystallinity. This phenomenon can be attributed to the interaction between organic functional groups and the $Fe_3O_4$ surface, which may lead to partial coverage of the magnetite crystallites.

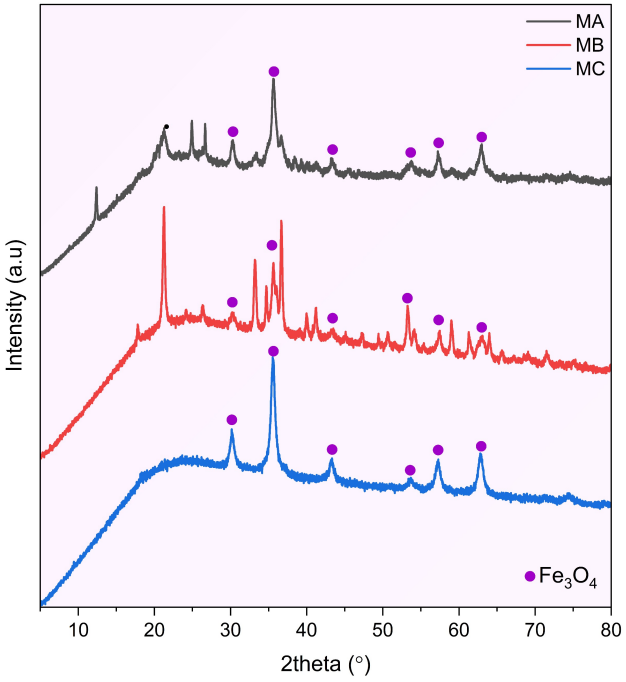


**Figure 1.** XRD Pattern of MgAl LDH/Lignin

The FTIR spectrum of magnetite exhibits distinct stretching vibrations associated with Fe−O and O−Fe−O bonds, observed at wavenumbers of 837 $cm^{-1}$ and 783 $cm^{-1}$, respectively. Additionally, stretching vibrations at 537 $cm^{-1}$ further corroborate the presence of a magnetite spinel structure (Gherca et al., 2022). The findings from the synthesis of magnetite alongside natural materials A, B, and C indicate a confluence of the spectral characteristics associated with the two precursors. The spectra of the carbon materials in Figure 2 exhibit a pronounced absorption band at approximately 3444 $cm^{-1}$, which is attributed to the O-H stretching vibrations associated with both phenolic and aliphatic alcohol functional groups (Wang et al., 2024). The absorption band observed at 2924 $cm^{-1}$ is indicative of CH stretching vibrations. In contrast, the absorption bands located at 1512 $cm^{-1}$ and 1604 $cm^{-1}$ correspond to C=C stretching vibrations associated with the aromatic structure (Palapa et al., 2023b; Adawiyah et al., 2024). The observed bands at 1134 $cm^{-1}$ and 1014 $cm^{-1}$ correspond to C−O stretching vibrations associated with methoxyl and alcohol functional groups (Li et al., 2023). Additionally, the absorption band observed at 617 $cm^{-1}$ is indicative of aromatic C−H hydrocarbons. The observed bands indicate that in samples MA, MB, and MC, magnetite exhibits interactions with organic materials via functional groups, while maintaining the spinel structure characteristic of magnetite alongside the principal functional groups present in the organic materials. The observed variations in intensity and the shifts in absorption bands following the preparation of the adsorbent suggest the occurrence of interactions between magnetite and the respective organic materials.

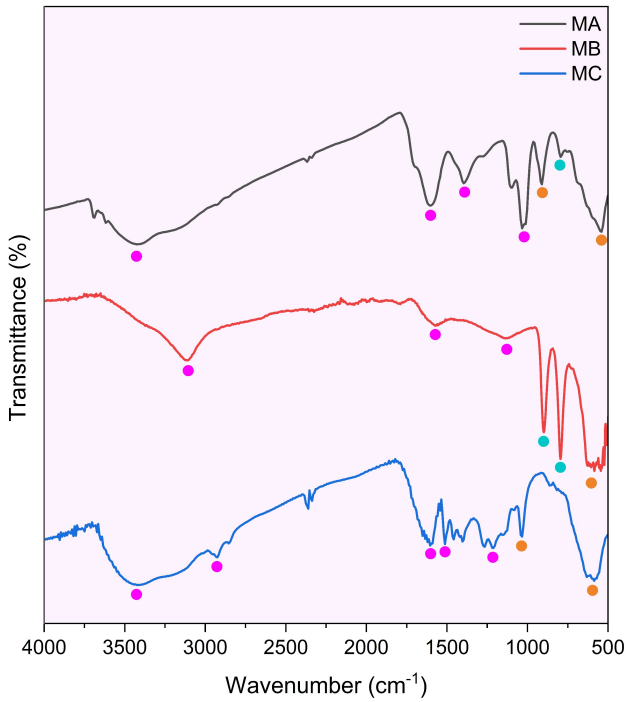


**Figure 2.** FTIR Spectra of MgAl LDH/Lignin

The surface analysis data, including BET and BJH measurements for samples MA, MB, and MC, are presented in Figure 3. The adsorbents MA, MB, and MC demonstrate a variety of pore characteristics. Magnetite exhibits a specific surface area of 68.338 $m^2/g$, a pore size measuring 18.027 nm, and a pore volume of 0.308 $cm^3/g$. The material demonstrates a Type IV isotherm alongside an H3 hysteresis loop, which signifies the existence of a mesoporous architecture characterized by slit-shaped pores (Silva et al., 2022). This specific isotherm and hysteresis loop phenomenon is similarly observed in MA and MC, whereas MB exhibits a Type I isotherm, characterized by the absence of a hysteresis loop (Ahmad et al., 2025). The MA, MB, and MC adsorbents exhibit specific surface areas ranging from 35.718 to 662.560 $m^2/g$, pore sizes between 2.758 and 20.413 nm, and pore volumes varying from 0.072 to 0.456 $cm^3/g$, respectively. MB exhibits the highest specific surface area and pore volume, alongside the smallest pore size when compared to MA and MC.

The pHpzc represents the pH level at which the charge of the adsorbent is neutral, serving as a critical parameter for understanding the surface charge equilibrium of the adsorbent (Mittal, 2021). The pHpzc is determined by identifying the intersection point between the initial pH curve and the final pH curve.

**Table 1.** Calculation of Adsorption Kinetics Models for MA, MB, and MC

| Material | PFO | | | | PSO | | |
|---|---|---|---|---|---|---|---|
| | $Q_{exp}$ (mg/g) | $Q_{calc}$ (mg/g) | $k_1$ ($min^{-1}$) | $R^2$ | $Q_{calc}$ (mg/g) | $k_2$ (g $mg^{-1}$ $min^{-1}$) | $R^2$ |
| MA | 19.551 | 18.893 | 0.039 | 0.983 | 22.727 | 0.002 | 0.987 |
| MB | 46.667 | 32.137 | 0.027 | 0.986 | 50.505 | 0.001 | 0.999 |
| MC | 9.615 | 7.124 | 0.029 | 0.901 | 10.091 | 0.011 | 0.999 |

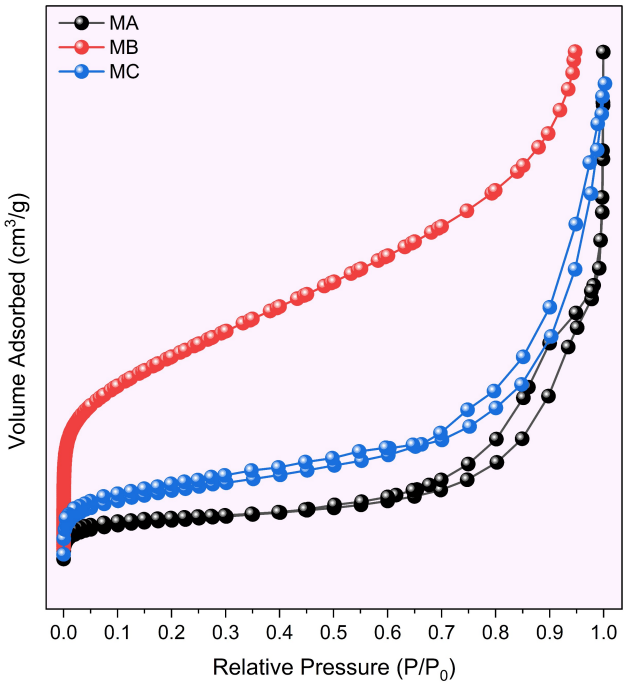


**Figure 3.** N2 Adsorption-Desorption of MgAl LDH/Lignin

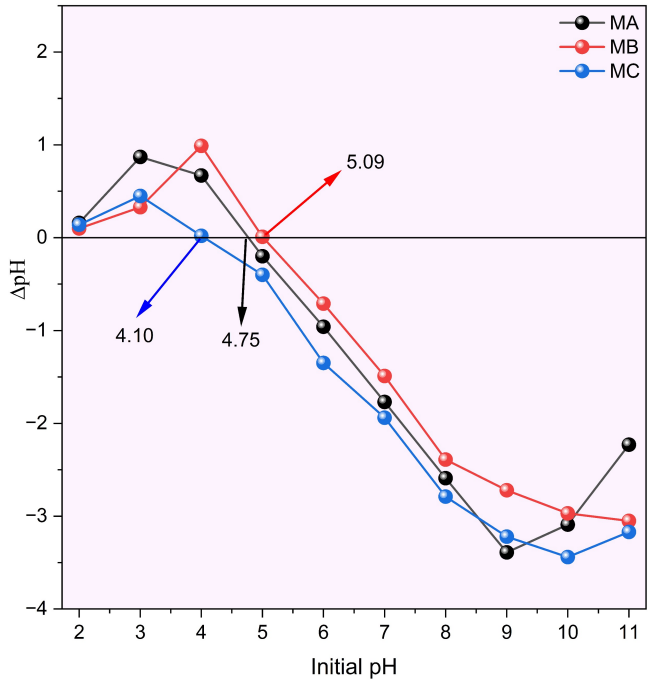


**Figure 4.** pHpzc of MA, MB, and MC Materials

The pHpzc values determined are approximately 4.75 for MA, 5.09 for MB, and 4.10 for MC (Figure 4). The observed values suggest a significant dependence of the surface charge of each adsorbent on the specific type of organic material associated with magnetite. The marginally elevated pHpzc of MB indicates that activated charcoal may enhance the basicity of the surface characteristics, potentially attributable to a reduced presence of acidic oxygenated functional groups and an increased graphitic content. In the present investigation, adsorption experiments were performed at the corresponding pHpzc values of the adsorbents. This approach was adopted to mitigate the effects of electrostatic interactions between the adsorbent surfaces and the dye molecules. At pHpzc, the net surface charge of the adsorbent approaches neutrality, indicating a balance between the positive and negative surface sites present. In this context, the adsorption of adsorbate is predominantly influenced by non-electrostatic mechanisms, including hydrogen bonding, $\pi$-$\pi$ interactions, and surface complexation between the functional groups of the dye and the active sites present on the adsorbent.

The effect of time factors on the adsorption capacity of PR onto the MA, MB, and MC is illustrated in Figure 5. The findings of the investigation demonstrate that the adsorption process of PR exhibits a decline in concentration over time, with the adsorption capacity reaching equilibrium at 120 min. The analysis of the PR adsorption kinetics data presented in Table 1 indicates that the adsorption process adheres to the PSO model. The superiority of the PSO model is demonstrated by its elevated correlation coefficient ($R^2$) value in comparison to the PFO model. Furthermore, the Qecalc value obtained from the PSO model exhibits a closer alignment with the experimental value (Qeexp) in comparison to the PFO model (Ai et al., 2025). This observation suggests that the underlying adsorption mechanism is primarily governed by chemical interactions rather than physical ones (He et al., 2025). The PSO model elucidates that the adsorption process is characterized by chemical interactions occurring between PR and the active sites present on the surface of the adsorbent. The presence of active groups on the adsorbent, including −OH, −COOH, and metal ions derived from magnetite, contributes to

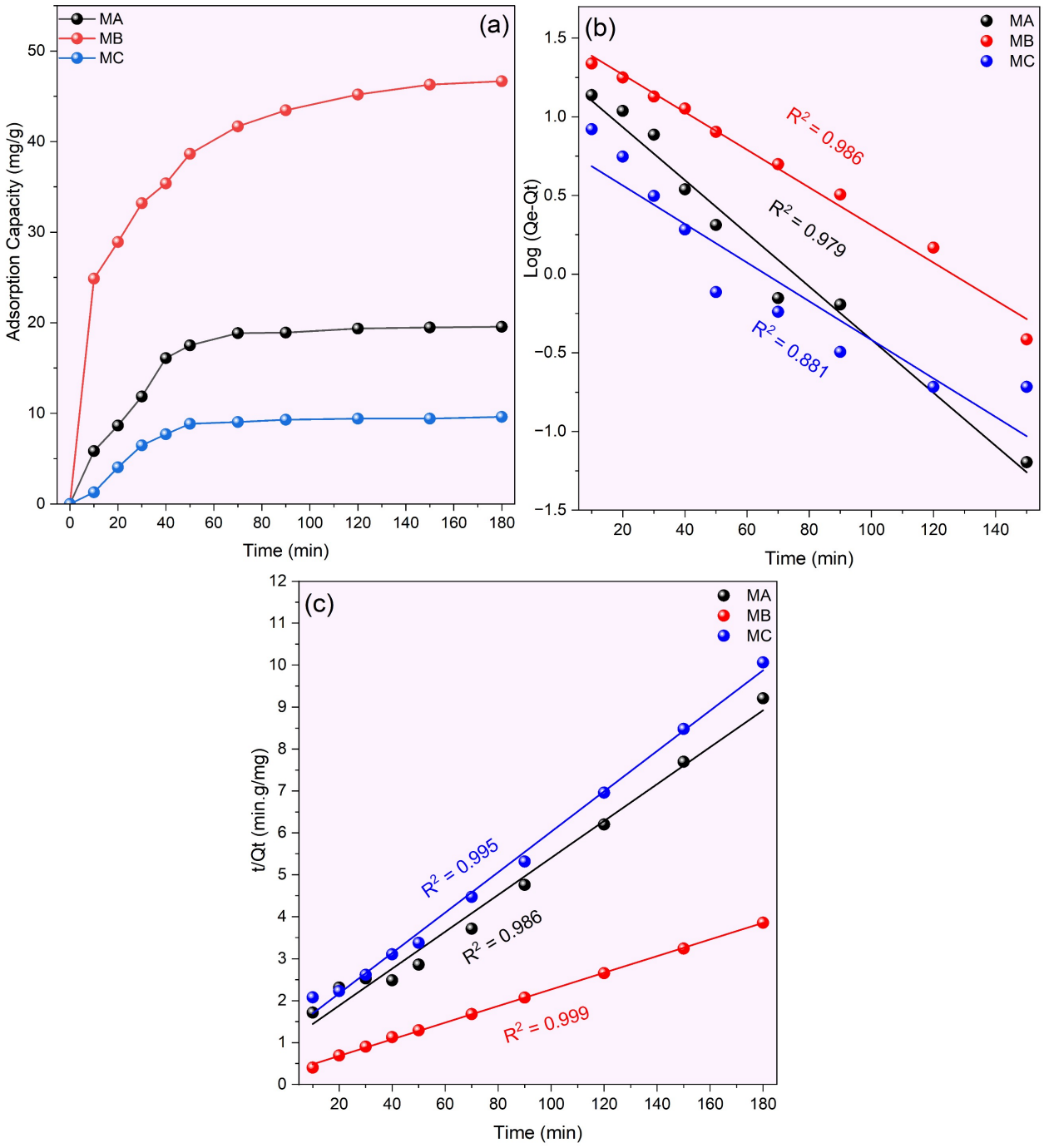


**Figure 5.** Effect of Time (a) and Its Kinetic Model: (b) PFO; (c) PSO) in Adsorption of PR

the formation of chemical bonds with sulfonate ($-SO_3^-$) or azo ($-N=N^-$) groups within the PR molecule.

The adsorption equilibrium data for PR on MA, MB, and MC were analyzed utilizing both the Langmuir and Freundlich isotherm models. The resulting parameters are detailed in Table 2. The $R^2$ indicate that the Langmuir model offers a superior fit for the majority of systems examined, implying that adsorption primarily takes place on a uniform surface characterized by monolayer coverage of dye molecules (Palapa et al., 2023a; Wijaya et al., 2023). The observed Langmuir maximum adsorption capacities ($Q_m$) exhibited an increase with rising temperature, suggesting that the adsorption process is inherently endothermic. Among the three adsorbents evaluated, MB demonstrated the $Q_m$ of 52.63 mg/g at a temperature of 50°C. This value is signifi-

**Table 2.** Adsorption Isotherm Models for MA, MB, and MC

| Adsorbent | $T$ (°C) | Langmuir | | | Freundlich | | |
|---|---|---|---|---|---|---|---|
| | | $Q_m$ (mg/g) | $k_L$ (mg/L) | $R^2$ | $n$ | $k_F$ | $R^2$ |
| MA | 30 | 1.560 | 0.045 | 0.982 | 1.386 | 5.757 | 0.873 |
| | 40 | 8.905 | 0.013 | 0.941 | 2.088 | 1.780 | 0.919 |
| | 50 | 6.502 | 0.046 | 0.979 | 4.658 | 1.993 | 0.755 |
| MB | 30 | 7.008 | 0.037 | 0.828 | 0.383 | 0.552 | 0.638 |
| | 40 | 9.579 | 0.048 | 0.985 | 0.492 | 2.866 | 0.977 |
| | 50 | 52.632 | 0.150 | 0.950 | 0.694 | 2.313 | 0.765 |
| MC | 30 | 6.079 | 0.022 | 0.970 | 0.960 | 24.110 | 0.934 |
| | 40 | 6.211 | 0.024 | 0.974 | 1.108 | 12.543 | 0.945 |
| | 50 | 6.998 | 0.019 | 0.958 | 1.151 | 10.488 | 0.955 |

cantly greater than those observed for MA (6.50 mg/g) and MC (6.99 mg/g). These findings indicate that the activated charcoal matrix offers an enhanced surface area and a greater availability of adsorption sites for the interaction with dye molecules.

The Freundlich constants ($n$ >1) for all materials indicate that the adsorption process is favorable and takes place on heterogeneous surfaces. The kF values exhibited an increase with rising temperature, thereby providing further evidence for the enhancement of adsorption at elevated thermal conditions. MC exhibited notably elevated kF values suggesting the presence of strong affinity sites associated with the aromatic and oxygen-containing functional groups inherent to lignin. The enhanced performance of MC in comparison to MA and MC is primarily due to its increased surface area, improved porosity, and more robust interaction between $Fe_3O_4$ and the activated carbon matrix. These factors contribute to a greater capacity for dye uptake and stability at elevated temperatures.

**Table 3.** Comparison of Maximum Adsorption Capacity with Previous Studies

| Adsorbent | $Q_m$ (mg/g) | References |
|---|---|---|
| MA | 8.905 | This work |
| MB | 52.632 | This work |
| MC | 31.949 | This work |
| Spirulina | 11.23 | (Mohadi et al., 2017) |
| AC of bagasse | 6.90 | (Fahira et al., 2021) |
| Rambutan peel | 182.40 | (Hasanah et al., 2022) |
| Montmorillonite | 11.04 | (Sarma et al., 2018) |
| Rice husk-BC | 84.034 | (Palapa et al., 2021) |
| Tamarind-seed testa | 61.1 | (Chaiyapongputti et al., 2014) |

The $Q_m$ values of the synthesized adsorbents were evaluated in comparison to those of materials documented in prior studies, as illustrated in Table 3. The better adsorption performance of MB can be primarily ascribed to the highly porous architecture and substantial surface area of activated charcoal, which facilitates an increased number of active sites for interaction with PR. The $Q_m$ values of the synthesized materials, while lower than those of certain reported adsorbents, demonstrate comparability or superiority relative to various conventional materials. The findings indicate that the integration of magnetite within natural carbon-based matrices significantly improves adsorption efficacy, while also providing magnetic characteristics that aid in the recovery and reusability of the adsorbent. Consequently, the synthesized magnetic composites emerge as viable candidates for the effective removal of anionic dyes, including PR, from aqueous environments.

## 4. CONCLUSIONS

This research underscores the innovative approach of creating magnetite-based hybrid adsorbents aimed at the effective removal of PR. The innovative aspect is characterized by the integration of magnetite nanoparticles with naturally derived organic matrices, such as humic acid, activated charcoal, and lignin. The performance of adsorption experiments at pHpzc for each material facilitated a comprehensive assessment of the intrinsic interactions occurring between the adsorbent surface and PR molecules, thereby eliminating the influence of electrostatic effects. Among the composites studied, magnetite activated charcoal demonstrated a markedly better adsorption performance than magnetite humic acid and magnetite lignin. This enhancement can be ascribed to its increased surface area, porosity, and improved dispersion of $Fe_3O_4$ particles within the carbon matrix. These findings underscore the significant influence of structural and chemical synergy between the magnetic and carbonaceous components. The predominance of the PSO kinetic model alongside the Langmuir isotherm indicates that the adsorption process is governed by chemisorption and takes place on uniform monolayer surfaces. The interplay among surface chemistry, porosity, and the incorporation of magnetite illustrates a viable approach for the development of economical, recyclable adsorbents derived from sustainable materials. This study significantly advances the field of magnetically separable adsorbents, specifically those derived from renewable carbonaceous materials, aimed at the treatment of textile wastewater.

## 5. ACKNOWLEDGEMENT

This research is supported by the Research Center of Inorganic Materials and Coordination Complexes, Universitas Sriwijaya.

## REFERENCES

Adawiyah, R., N. Yuliasari, Y. Hanifah, K. Alawiyah, and N. Rahayu Palapa (2024). Utilizing *Areca catechu* L. Fruit Peel-Derived Biochar and Hydrochar for Congo Red Adsorption: Kinetic and Thermodynamic Analysis. *Indonesian Journal of Environmental Management and Sustainability*, **8**(4); 135–144

Ahmad, N., T. Kameda, M. T. Rahman, F. Rahman, and A. Lesbani (2025). Preparation of a New Hybrid MgAlLDH@Magnetite Activated Charcoal by Hydrothermal Method for Stability and Adsorption Mechanism of Congo Red. *Results in Surfaces and Interfaces*, **18**; 100440

Ahmad, N., Rohmatullaili, A. Wijaya, and A. Lesbani (2024). Magnetite Humic Acid-Decorated MgAl Layered Double Hydroxide and Its Application in Procion Red Adsorption. *Colloids and Surfaces A: Physicochemical and Engineering Aspects*, **684**; 133042

Ai, S., K. Gao, L. Liu, and W. Yu (2025). Quasi-Homogeneous Adsorption Behavior of a Magnetic Iron-Based Hydrated Material for Congo Red. *Environmental Technology and Innovation*, **40**; 104362

Ain, Q. U., U. Rasheed, Z. Chen, R. He, and Z. Tong (2024). Activation of $Fe_3O_4$/Bentonite Through Anchoring of Highly Dispersed and Photo-Reduced Cu Ions for Higher pH Fenton-Like Degradation and Effective Adsorption of Congo Red Dye. *Journal of Industrial and Engineering Chemistry*, **134**; 327–342

Amri, A., Z. A. Zahara, P. M. S. B. N. Siregar, Z. Zulkarnain, and A. Wijaya (2024). Synthesis and Characterization of Ni/Al Layered Double Hydroxides Composite Based-Material with Chitosan, Cellulose, and Graphene Oxide. *Indonesian Journal of Material Research*, **2**(1); 27–31

Anuar, F. I., T. Hadibarata, M. Syafrudin, and Z. Fona (2020). Removal of Procion Red MX-5B from Aqueous Solution by Adsorption on *Parkia speciosa* (Stink Bean) Peel Powder. *Biointerface Research in Applied Chemistry*, **10**(1); 4774–4779

Ayesha, M. Imran, A. Haider, I. Shahzadi, S. Moeen, A. Ul-Hamid, W. Nabgan, A. Shahzadi, T. Alshahrani, and M. Ikram (2023). Polyvinylpyrrolidone and Chitosan-Coated Magnetite (Fe3O4) Nanoparticles for Catalytic and Antimicrobial Activity with Molecular Docking Analysis. *Journal of Environmental Chemical Engineering*, **11**(3); 110088

Chaiyapongputti, P., P. Sae-Bae, J. Setthayanond, and P. Munsuwan (2014). Development of Adsorbent Material from Tamarind-Seed Testa for Reactive Dye Adsorption. *Applied Mechanics and Materials*, **535**; 650–653

Cotillas, S., J. Llanos, P. Cañizares, D. Clematis, G. Cerisola, M. A. Rodrigo, and M. Panizza (2018). Removal of Procion Red MX-5B Dye from Wastewater by Conductive-Diamond Electrochemical Oxidation. *Electrochimica Acta*, **263**; 1–7

dos Santos, G. E. d. S., P. V. d. S. Lins, L. M. T. d. M. Oliveira, E. O. d. Silva, I. Anastopoulos, A. Erto, D. A. Giannakoudakis, A. R. F. d. Almeida, J. L. d. S. Duarte, and L. Meili (2021). Layered Double Hydroxides/Biochar Composites as Adsorbents for Water Remediation Applications: Recent Trends and Perspectives. *Journal of Cleaner Production*, **284**; 124755

Fahira, C. A., D. R. Damayanti, A. Febrianti, and R. A. S. Lestari (2021). Adsorb Red Procion in Batik Waste Used Baggase Adsorbent. In *AIP Conference Proceedings*, volume 2349. page 020069

Gherca, D., A. I. Borhan, M. M. Mihai, D. D. Herea, G. Stoian, T. Roman, H. Chiriac, N. Lupu, and G. Buema (2022). Magnetite-Induced Topological Transformation of 3D Hierarchical MgAl Layered Double Hydroxides to Highly Dispersed 2D Magnetic Hetero-Nanosheets for Effective Removal of Cadmium Ions from Aqueous Solutions. *Materials Chemistry and Physics*, **284**; 126047

Hasanah, M., N. Juleanti, A. Priambodo, F. S. Arsyad, A. Lesbani, and R. Mohadi (2022). Utilization of Rambutan Peel as a Potential Adsorbent for the Adsorption of Malachite Green, Procion Red, and Congo Red Dyes. *Ecological Engineering and Environmental Technology*, **23**(3); 148–157

He, J., L. Zhu, S. Guo, and B. Yang (2025). An Effective Strategy for Coal-Series Kaolin Utilization: Preparation of Magnetic Adsorbent for Congo Red Adsorption. *Chemical Engineering Science*, **304**; 120958

Hingrajiya, R. D. and M. P. Patel (2023). Fe3O4 Modified Chitosan Based Co-Polymeric Magnetic Composite Hydrogel: Synthesis, Characterization and Evaluation for the Removal of Methylene Blue from Aqueous Solutions. *International Journal of Biological Macromolecules*, **244**; 125251

Iqajtaoune, A., M. Taibi, H. Saufi, B. Aouan, and L. Boudad (2024). Enhanced Removal of Methylene Blue and Procion Deep Red H-EXL Dyes from Aqueous Environments by Modified-Bentonite: Isotherm, Kinetic, and Thermodynamic. *Desalination and Water Treatment*, **320**; 100607

Kalidason, A. and T. Kuroiwa (2022). Synthesis of Chitosan–Magnetite Gel Microparticles with Improved Stability and Magnetic Properties: A Study on Their Adsorption, Recoverability, and Reusability in the Removal of Monovalent and Multivalent Azo Dyes. *Reactive and Functional Polymers*, **173**; 105220

Li, S., X. Li, S. Li, P. Xu, Z. Liu, and S. Yu (2024). In-Situ Preparation of Lignin/Fe3O4 Magnetic Spheres as Bifunctional Material for the Efficient Removal of Metal Ions and Methylene Blue. *International Journal of Biological Macromolecules*, **259**; 128971

Li, W., L. Chai, B. Du, X. Chen, and R. C. Sun (2023). Full-Lignin-Based Adsorbent for Removal of Cr(VI) from Waste Water. *Separation and Purification Technology*, **306**; 122644

Mittal, J. (2021). Recent Progress in the Synthesis of Layered Double Hydroxides and Their Application for the Adsorptive Removal of Dyes: A Review. *Journal of Environmental Management*, **295**; 113017

Mohadi, R., Z. Hanafiah, H. Hermansyah, and H. Zulkifli (2017). Adsorption of Procion Red and Congo Red Dyes Using Microalgae Spirulina sp. *Science and Technology Indonesia*, **2**(4);

 

102–104
Mohd Nor, N., T. Hadibarata, Z. Yusop, and Z. M. Lazim (2015). Removal of Brilliant Green and Procion Red Dyes from Aqueous Solution by Adsorption Using Selected Agricultural Wastes. *Jurnal Teknologi*, **74**(11); 117–122
Naik, V. A. and V. A. Thakur (2024). Hydrothermal Synthesis of Fe3O4@rGO@CdS/Bi2S3 Nanocomposite as an Efficient, Recyclable Magnetic Photocatalyst for Photo-Fenton Dye Degradation and Chromium VI Reduction under Sunlight. *Inorganic Chemistry Communications*, **160**; 111962
Palapa, N. R., N. Ahmad, A. Wijaya, and Z. A. Zahara (2023a). Facile Fabrication of Layered Double Hydroxide-Lignin for Efficient Adsorption of Malachite Green. *Science and Technology Indonesia*, **8**(2); 305–311
Palapa, N. R., Y. Hanifah, Amri, and B. I. Putri (2023b). Comparative Study of Biochar and Hydrochar Derived from Agricultural Waste: Characterization and Chemical Properties. *Indonesian Journal of Environmental Management and Sustainability*, **8**(1); 34–38
Palapa, N. R., T. Taher, N. Juleanti, Normah, and A. Lesbani (2021). Biochar from Rice Husk as Efficient Biosorbent for Procion Red Removal from Aqueous Systems. *Applied Environmental Research*, **43**(3); 79–91
Palapa, N. R. and A. Wijaya (2023). Layered Double Hydroxide Coated by Carbon-Based Material for Environmental Dye Pollutant. *Indonesian Journal of Material Research*, **1**(3); 84–90
Palas, B., G. Ersöz, and S. Atalay (2016). Heterogeneous Photo Fenton-Like Oxidation of Procion Red MX-5B Using Walnut Shell Based Green Catalysts. *Journal of Photochemistry and Photobiology A: Chemistry*, **324**; 165–174
Ribas, M. C., M. A. E. de Franco, M. A. Adebayo, E. C. Lima, G. M. B. Parkes, and L. A. Feris (2020). Adsorption of Procion Red MX-5B Dye from Aqueous Solution Using Homemade Peach and Commercial Activated Carbons. *Applied Water Science*, **10**(6); 1–13
Salman, M., M. Demir, K. H. D. Tang, L. T. T. Cao, S. Bunrith, T.-W. Chen, N. M. Darwish, B. M. AlMunqedhi, and T. Hadibarata (2022). Removal of Cresol Red by Adsorption Using Wastepaper. *Industrial and Domestic Waste Management*, **2**(1); 1–8
Sarma, G. K., S. SenGupta, and K. G. Bhattacharyya (2018). Adsorption of Monoazo Dyes (Crocein Orange G and Procion Red MX5B) from Water Using Raw and Acid-Treated Montmorillonite K10: Insight into Kinetics, Isotherm, and Thermodynamic Parameters. *Water, Air, and Soil Pollution*, **229**(10); 312
Silva, T. S., E. P. Fernandes, M. Vithanage, S. M. P. Meneghetti, and L. Meili (2022). A Facile Synthesis of MgAl/Layered Double Hydroxides from Aluminum Wastes. *Materials Letters*, **324**; 132624
Tao, P. and Y. Wang (2023). Enhanced Photocatalytic Performance of W-Doped TiO2 Nanoparticles for Treatment of Procion Red MX-5B Azo Dye in Textile Wastewater. *International Journal of Electrochemical Science*, **18**(9); 100261
Thue, P. S., R. A. Teixeira, J. W. Hounfodji, F. M. Machado, B. L. Mello, R. Andreazza, M. Naushad, Y. Dehmani, M. Badawi, and E. C. Lima (2024). Intercalation of Organosilane in Clay Mineral for the Removal of Procion Red MX-5B: Investigational and Theoretical Studies. *Separation and Purification Technology*, **347**; 127491
Wang, P., C. Chen, M. Chen, J. Wei, Y. Lan, X. Lu, and Z. Huang (2024). Facile and Green Synthesis of Lignin-Based Aggregate Microparticles Adsorbent with Hydrothermal Regeneration Function for Ciprofloxacin Removal from Water. *Journal of Environmental Chemical Engineering*, **12**(2); 112207
Wijaya, A., P. Mega, S. Bahar, N. Siregar, A. Priambodo, N. R. Palapa, T. Taher, and A. Lesbani (2021). Innovative Modified of Cu-Al/C (C = Biochar, Graphite) Composites for Removal of Procion Red from Aqueous Solution. *Science and Technology Indonesia*, **6**(4); 228–234
Wijaya, A., P. M. S. B. N. Siregar, A. F. Badri, N. R. Palapa, A. Amri, N. Ahmad, and A. Lesbani (2023). Modified Layered Double Hydroxide Mg/M3+ (M3+ = Al and Cr) Using Metal Oxide (Cu) as Adsorbent for Methyl Orange and Methyl Red Dyes. *Periodica Polytechnica Chemical Engineering*, **67**(2); 173–184

 